


Preparation and physical characteristics of epoxy resin/bacterial cellulose biocomposites

Sinh Le Hoang¹ · Cuong Manh Vu^{2,3}  ·
Lanh Thi Pham⁴ · Hyoung Jin Choi⁵

Received: 8 March 2017 / Revised: 26 July 2017 / Accepted: 18 August 2017 /
Published online: 4 September 2017
© Springer-Verlag GmbH Germany 2017

Abstract Using bacterial cellulose (BC) prepared from Vietnamese nata-de-coco via an alkaline pre-treatment followed by a solvent exchange process, epoxy resin (EP)/BC biocomposites were fabricated using three different dispersion techniques: mechanical stirring only, both mechanical stirring and grinding, and both mechanical stirring and ultrasonication. The surface of BC was modified with a silane coupling agent to improve the chemical affinity between BC and epoxy resin. The biocomposite materials comprising BC, epoxy resin, and methylhexahydrophthalic anhydride as a curing agent were obtained from hot curing processing. The morphology and mechanical properties such as fracture toughness, enhanced K_{IC} values, and tensile and flexural properties of the bio-based composites were compared with those of the virgin epoxy resin. The silane coupling agent had a vital role in improving the mechanical characteristics of the bio-based composites. For instance, K_{IC} values, tensile strength, Young's modulus, and flexural strength of the 0.3 wt% BC/epoxy composites with the presence of 2.0 wt% silane coupling agent were 0.7740 MPa m^{1/2}, 53.32 MPa, 1.68 GPa, and 83.05 MPa. These values represent improvements of 36.77, 17, 15.86, and 14.42%, respectively, compared to a neat epoxy resin. Scanning electron microscopy revealed the rough fracture surface

✉ Cuong Manh Vu
vumanhcuong1@tdt.edu.vn

¹ Center for Advanced Chemistry, Institute of Research and Development, Duy Tan University, Da Nang, Vietnam

² Department for Management of Science and Technology Development, Ton Duc Thang University, Ho Chi Minh City, Vietnam

³ Faculty of Applied Sciences, Ton Duc Thang University, Ho Chi Minh City, Vietnam

⁴ Viet Nam Academy of Science and Technology, Ha Noi, Vietnam

⁵ Department of Polymer Science and Engineering, Inha University, Incheon 402-751, Korea

of epoxy resin/BC-based biocomposites with a multipathway crack, requiring more energy before breakage.

Keywords Epoxy resin · Bacterial cellulose · Bio-based composite · Nata-de-coco · Mechanical property · Fracture toughness

Introduction

Along with the huge development of polymer-based composite materials, many kinds of reinforcement materials, such as glass fiber [1], carbon fiber [2], and Kevlar [3] have been used for composites with great improvements in the mechanical properties. On the other hand, all of these usually come from chemical industries through chemical synthesis or from petroleum sources, causing a range of environmental problems during their synthesis and uses. In recent years, researchers have paid more attention to finding new materials with renewable and biodegradable features due to a decrease in non-renewable resources and environmental concerns [4]. In addition, the use of renewable resources has brought many economic advantages at low cost compared to non-renewable resources. In this context, a re-enforcer with cost-effective and sustainable resources can replace industrial resource-based fillers. Cellulose is the most renewable and abundant natural biopolymeric resource on Earth [5]. Among its various sources, bacterial cellulose (BC) is a type of biological resource [6] that can be used as a filler for biocomposite fabrication. BC exists in one kind of coconut palm product, called nata-de-coco.

In Vietnam, coconut palms are planted widely in all regions of the Mekong Delta, especially in Ben Tre Province, which is called the capital of coconut production [7]. Coconut water is also the most valuable product of the coconut palm and many applications, such as beverages or for the production of nata-de-coco. Nata-de-coco is produced from coconut water medium enriched with carbon and nitrogen through fermentation processing using genera *Acetobacter* bacteria [8]. Under such conditions, nanosized BC fibrils are secreted through *Acetobacter* bacterial cell wall [9], with dimension of 70–100 nm in width and several micrometers in length. Nanosized BC fibers are characterized by the high water holding capacity, high hydrophilicity due to many hydroxyl groups located in their structure, high crystallinity (due to no other ingredients such as lignin and hemicellulose in comparison to plant cellulose), and high strength and modulus with very large specific surface area [10]. Furthermore, owing to its excellent properties, BC has become an essential part of the biocomposite materials based on different kinds of resins, such as epoxy [11, 12], PLA [13, 14], and PVA [15, 16], with significant enhancement of their mechanical properties. Epoxy resin, as one of the most important thermoset resins, possesses many favorite features, such as high strength, high modulus, good chemical resistance, and compatibility with various kinds of fillers. For this reason, epoxy resin is used widely in various industrial applications, such as marine [17], automobile, airplane [18], and medical devices. On the other hand, owing to its high cross-linking density, the epoxy resin has many serious

drawbacks in terms of brittleness or poor crack resistance at normal condition testing, which limits its applications to areas requiring high mechanical strength. Therefore, many studies have focused on enhancing the fracture toughness of epoxy resin. The common methods are either chemical modification to make the epoxy chain longer [19] or incorporation of hard particles [20, 21], thermoplastics [22], and nanofiber [23]. Among these, Liu et al. [24] used nanosilica–rubber core–shell nanoparticles to achieve 39.4% improvement of the impact strength at a 2 wt % loading. They also showed that the main causes for this phenomenon are crazing, microcracks formation, and debonding of nanoparticles from the matrix. Ladani et al. [25] used aligned carbon nanofibers to improve both the toughness and electrical conductivity of epoxy resin based nanocomposites. Vu et al. [19] reported that adducts obtained from thiokol showed improved fracture toughness of both epoxy resin and epoxy-based composite materials, because the epoxy chains are longer and more flexible and also reduce the degree of cross-linking. In this content, the BC nanosized fibrils were chosen as a toughening agent to overcome the inherent brittleness of epoxy networks because of its abundant availability, low cost and high mechanical strength. Apart from it, various filler/polymer composites with enhanced properties have been synthesized through different methodologies. Boland et al. [26] fabricated high stiffness nanocomposite fibers from polyvinyl alcohol filled with graphene and boron nitride by coagulation spinning using polyvinyl alcohol as a matrix. Son et al. [27] studied the compatibility of thermally reduced graphene (TRG) with multiblock copolyesters, composed of poly(butylene terephthalate) (PBT) segments and poly(tetramethylene ether) glycol segments. Reddy et al. [28] successfully synthesized the poly(*ortho*-toluidine) (POT)–gold (Au) and palladium (Pd) composite nanospheres by the reaction of *o*-toluidine with the corresponding metal (Au or Pd) colloidal solution through the self-assembly process in the presence of dodecylbenzenesulfonic acid (DBSA), which acts as both a dopant and surfactant, and ammonium peroxydisulfate as an oxidizing agent. Han et al. [29] fabricated the graphene modified lipophilically by stearic acid and its composite with low density polyethylene. Reddy et al. [30] have an overview about hybrid nanostructures based on titanium dioxide for enhanced photocatalysis. In another work, Reddy et al. [31] report the synthesis of conducting polyaniline-functionalized multi-walled carbon nanotubes (MWCNTs-f-PANI) containing noble metal (Au and Ag) nanoparticle composites (MWCNTs-f-PANI-Au or Ag-NC). MWCNTs-f-PANI. Reddy et al. [32] fabricated the nanostructured titanium dioxide/polyaniline hybrid with enhanced photocatalytic activity. Khan et al. [33] synthesized carbon nanotube (CNT) composites in a colloidal system with poly(styrene) or PS to form a nanostructured brush.

Although BCs have been used as effective and sustainable filler for epoxy resin using difference dispersion method, to the best of our knowledge the comparison between dispersion methods using mechanical stirrer only, both mechanical and grinding and both mechanical and ultrasonic have been seldom reported. The solvent exchange method used to prepare the solution of BC in ethanol is considered to be new. The current study focuses on the preparation and characterization of bio-based composite materials from epoxy resin and BC. A suspension of BC in ethanol was used as a bio-filler source to prepare EP/BC mixtures. The (3-

glycidylxypropyl)trimethoxy silane coupling agent (GS) was also added along with a suspension of BC in ethanol into the epoxy resin to enhance the stability of BC in the epoxy matrix. The mechanical properties, such as tensile properties, flexural properties, and fracture toughness of bio-based composite materials, are greatly affected by the dispersion of fillers, and their interfacial interactions with epoxy resin were investigated.

Experimental

Materials

Nata-de-coco used as a bacterial cellulose source was obtained from Dang Khoa coconut company, Ben Tre Province, Vietnam with a 10 wt% dry content (90 wt% of nata-de-coco is water). Epoxy resin (trade name Epikote828, epoxy content = 22.63%, molecular weight ~ 383 g/mol, viscosity = 12–13 Pa s, density = 1.16 g/cm³ at 25 °C) was supplied by Shell Chemical. Methylhexahydrophthalic anhydride (MHHPA) procured from Jiaying Alpharm Fine Chemical Co., China, was used as the curing agent. 1-Metylimidazol (NMI) and polyol (BASF, Germany) was used as the accelerators. (3-Glycidylxypropyl)trimethoxysilane (GS) was purchased from Sigma-Aldrich. Ethanol and acetone were used as the solvent without further purification.

Methods of BC dispersion in epoxy resin

Initially, the suspension of 20 wt% BC in ethanol was prepared from nata-de-coco by combining two processes of an alkaline pre-treatment followed by a water exchange process. The aim of this processing is to replace water in nata-de-coco with ethanol. First of all, nata-de-coco was maintained in a 2.5 M NaOH solution for 8 h at room temperature to remove the bacterial cells, followed by washing with distilled water until neutralization. The alkaline pre-treated nata-de-coco was well blended using a food mixer for 20 min to obtain a cellulosic pulp. In the next step, the water in the slurry was removed using a vacuum filter before obtaining the BC sheet containing approximately 80 wt% water and 20 wt% BC. Subsequently, the BC sheet was immersed in ethanol and blended using a food mixer for 20 min and filtered with the help of a vacuum filter. This processing was repeated three times before producing the suspension of 20 wt% BC in ethanol. The obtained suspension

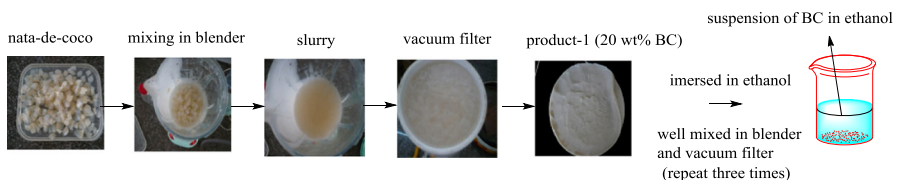


Fig. 1 Preparation of the suspension of 20 wt% BC in ethanol

was used for the preparation of EP/BC mixtures as well as bio-based composite materials. Figure 1 shows the details of this processing.

In this study, three different dispersion methods were used to incorporate BC in the epoxy resin, in which the BC contents were in the range 0–0.4 wt% with respect to the mass of epoxy resin. As the first mixing method of using a high speed mechanical stirrer only (MS), the epoxy resin was processed in an Ultra-Turrax homogenizer (IKA–werne/T50 basic/S50 N–G45G) at 2000 rpm for 20 min at 70–80 °C, followed by the slow addition of the suspension of 20 wt% BC in ethanol until the required BC content was reached. The time for this processing took 5 h. Subsequently, the ethanol was removed completely from the mixture using a vacuum oven at 60 °C for 3 h before curing processing.

The second mixing method uses both a high speed mechanical stirrer and grinder. First, the suspension of BC in ethanol was calculated and dispersed in epoxy resin using a high speed mechanical stirrer at 2000 rpm, at 70–80 °C for 5 h. Subsequently, the obtained mixture was ground at 400 rpm for 720 min using a grinder, and the ethanol in the mixture was removed completely using a vacuum oven at 60 °C for 3 h.

For the third method, the dispersion of BC in epoxy resin was mixed using a high speed mechanical stirrer and ultrasonic technique. Initially, the suspension of BC in ethanol was dispersed in epoxy resin using a high speed mechanical stirrer at 2000 rpm, at 70–80 °C for 5 h. Subsequently, the resulting mixture was agitated by ultrasonication for 30 or 60 min. An ice bath was also used in this step to prevent the evaporation of ethanol. Finally, the ethanol in the mixtures was removed completely using a vacuum oven at 60 °C for 3 h.

Preparation of bio-base composite materials

The epoxy resin was well mixed with a curing agent of MHPA (molar ratios of MHPA/EP change in the range from 0.8 to 1.01), accelerators of NMI and polyol (1.5 wt% with respect to the total mass of the MHPA/EP mixture) at 60 °C for 60 min using a magnetic stirrer. The mixture was degassed, poured into a mold coated with a release agent and cured in a vacuum oven via two steps: at 80 °C for 60 min followed by 100 °C for 60 min. Similar procedures were used to prepare the bio-based composite materials containing 0.1, 0.2, and 0.3 wt% BC in the epoxy resin.

Characterization

The degree of crystallinity (%) of BC was analyzed by X-ray diffraction (XRD) on a theta–theta type XRD-D8 ADVANCE, Bruker (Germany) using Cu-radiation generated at a voltage of 40 kV and a current of 40 mA with a D/texUltra detector. The scan range was 10°–50° 2 θ . The crystallinity index of BC was determined by the XRD peak height method using the following equation [34]:

$$X_{\text{cr}} = \frac{I_{002} - I_{\text{am}}}{I_{002}}, \quad (1)$$

where I_{002} is the maximum intensity of the peak corresponding to the plane with Miller indices of 002 and I_{am} is the minimal peak intensity of the diffraction of the amorphous phase at $18^\circ 2\theta$.

The thermal stability of both the treated and untreated BC was examined by thermogravimetric analysis [TGA, Setaram TG (France)]. The samples (~ 5 – 8 mg) were heated in air from 30 to 600 °C at a heating rate of 10 °C min⁻¹.

The gel content of the cured samples, which is represented as the undissolved part of the sample, was determined using a Soxhlet extractor and acetone as the solvent. The process included multi-steps. First, the filter paper was extracted in acetone for 20 h to remove the dissolved parts. Subsequently, the extracted filter papers were dried until a constant mass was obtained and weighed (*c*). The samples were packed and weighed with dried extracted filter paper (*b*) and extracted with acetone for 20 h. The samples after being extracted with acetone were dried and weighed again (*a*). The gel content (*X*) was calculated using the following equation:

$$X = \frac{a - c}{b - c} \times 100\%, \quad (2)$$

where *a* is the weight in grams of extracted samples including filter paper, *c* the weight in grams of the extracted filter paper, and *b* the weight in grams of the pristine samples including the filter paper. The relationship between the gel content and curing rate versus curing time was also calculated. The morphology of the fracture surface of both the virgin epoxy and bio-based composite materials was examined by scanning electron microscopy (SEM, S-4800 Hitachi, Japan). The samples were coated with a ~ 5 nm Pt overlayer to avoid charge accumulation during electron irradiation.

Regarding their mechanical characterization, both the tensile and flexural properties were measured using a mechanical tester (INSTRON 5582-100KN, USA) at 25 ± 2 °C and $60 \pm 5\%$ RH at a crosshead speed of 2 mm min⁻¹ according to the ISO 527 and ISO 178 standards, respectively. Five specimens for each type of bio-based composite material were measured. IZOD notched impact strength tests were also carried out on a Tinius Olsen Model 92T Plastic Impact (USA) impact tester in accordance with ISO 180. The measurements were taken at 25 ± 2 °C and $60 \pm 5\%$ RH. The data correspond to the average value of at least five specimens. The fracture toughness of all cured samples was evaluated using the critical stress intensity factor (K_{IC}) according to the ASTM D5045-99 standard by single-edge-notched (SEN) tests in a flexural three-point bending setup. Testing analysis was performed using a Lloyd 500N machine. The dimensions of the single-edge notch specimen (SEN) were approximately $30 \times 6 \times 3$ mm with an initial notch length of approximately 2.54 mm. The specimen was then slid with a fresh razor blade to generate cracks. The span length was set to 24 mm, which is approximately four times the width of the specimen, and the load was applied with a crosshead speed of 10 mm min⁻¹.

Results and discussion

The effects of the alkaline pre-treatment on the surface and thermal stability of BC were considered. The newly synthesized nata-de-coco contained a very low dry content (2–4 wt%) and its most part is water. To easily store and transport it, the water content in nata-de-coco needs to be removed using a pressing method. After this processing, the water content in nata-de-coco was approximately 90 wt% and it was cut into smaller pieces, as shown in Fig. 1.

The nata-de-coco was maintained in an NaOH solution to remove the remaining bacterial cell wall and any other chemicals. The effects of the alkaline pre-treatment on the morphology and dimensions of BC were evaluated from the SEM images of dried BC film, as shown in Fig. 2.

Figure 2 shows that the bacterial cell wall still existed in the untreated BC film with an individual or aggregation state, 2–4 μm long, which needs to be removed from the BC film for further analysis. At high magnification (10,000 \times), it can be observed easily that the BC exists in long fibers with a diameter of a few nanometers to several tens of nanometers and interlaced to form a web-shaped network structure.

On the other hand, the SEM of alkali-treated BC showed no bacterial cell wall and the surface of the fibers appeared cleaner. By comparison, the SEM image of the untreated BC film with the pre-treated BC film at the same magnification shows that the diameter of the alkali pre-treated BC fibers was approximately about few nanometers to several tens nanometers and there was no difference. Based on the results above, the vital role of the alkali pre-treatment is to remove the bacterial cell wall and clean the fiber surface without affecting the dimensions of the BC fiber.

Regarding the thermal properties of the samples, Figs. 3 and 4 show the TGA and DTG curves of both the untreated and alkaline pre-treated BC.

As shown in Fig. 3, the temperatures at which untreated BC reached the maximum weight loss (~ 64.8 wt%) (T_{max}) and almost entire decay (T_{all}) were 355.5 and 484.8 $^{\circ}\text{C}$, respectively. In contrast, the T_{max} and T_{all} values of the alkali pre-treatment BC were 361.4 and 490.7 $^{\circ}\text{C}$, respectively. The decomposition

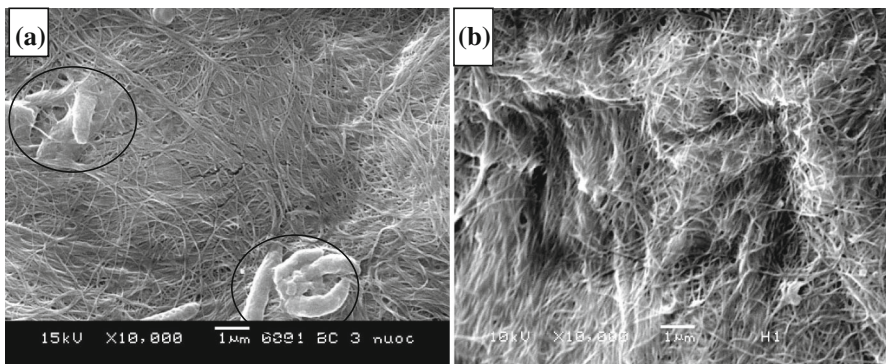


Fig. 2 SEM images of **a** untreated BC, **b** alkali-treated BC

Fig. 3 TGA of untreated and alkali-treated BC

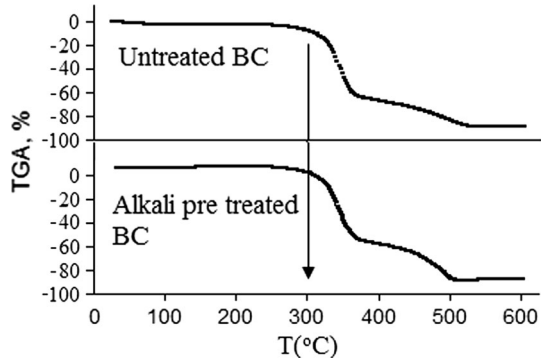
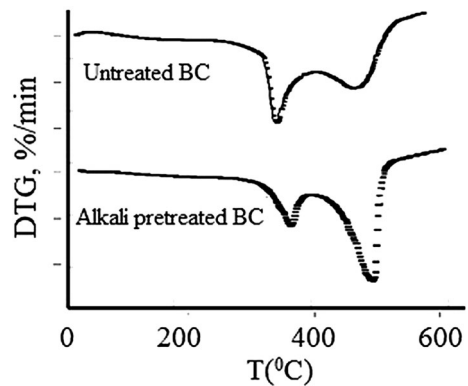


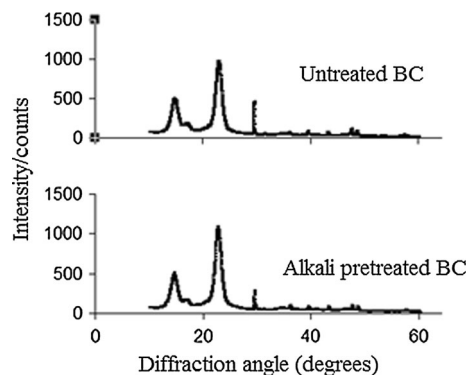
Fig. 4 DTG of untreated and alkali pre-treated BC



temperature of the alkali pre-treated BC was slightly higher than that of the untreated BC due to the removal of some volatile components as well as bacterial cell wall after this processing.

The crystal structure and degree of crystallinity of both the untreated and alkali pre-treated BC were examined by XRD, as presented in Fig. 5.

Fig. 5 XRD patterns of untreated and alkali-pre-treated BC



Both the untreated and alkali pre-treated BC showed peaks at 18.5 and 22.6° 2 θ with a similar height. The calculated degree of crystallinity of the untreated and alkali pre-treated BC were 91.06 and 91.34%, respectively. These results showed that alkali pre-treatment processing had no additional effects on both the crystalline state and the degree of crystallinity of BC.

On the other hand, the distribution and the existent state of BC in the epoxy resin strongly affect both the mechanical characteristics and the morphology of the bio-based composite materials, depending on the dispersion method treatment. Three different methods have been applied: using (MS) mechanical stirrer only, (MS + G) both mechanical stirrer and grinder treatment, and (MS + U) by combining mechanical stirrer and ultrasonics for the incorporation of BC in the epoxy matrix. To enhance the compatibility and avoid the aggregation of BC in the epoxy resin, the hydrophilic surface of BC was treated with a (3-glycidyloxypropyl) trimethoxy silane (GS) coupling agent co-added with a suspension of BC in ethanol into the epoxy resin. The role of GS on the dispersion of BC in epoxy resin was evaluated by SEM. Figure 6 shows the SEM images of the uncured EP/BC film produced using a mechanical stirrer for 300 min.

The SEM images of uncured epoxy/BC film in the presence of GS (Fig. 6b) showed a better distribution of BC fibers in the epoxy compared to the uncured epoxy/BC in the absence of GS (Fig. 6a). In the absence of GS, the BC fibers aggregated as result of the lesser compatibility between BC and epoxy resin, and high hydroxyl groups existed on the BC surface and H bond. In the next step, after 300 min with a mechanical stirrer treatment, the BC/epoxy mixtures in the presence of GS were treated further with either a grinder or ultrasonic technique. Figure 7 shows the effects of the dispersion treatment methods on the optical transparency of the BC/EP films.

The results show that the optical transparency of the uncured BC/EP film treated with a mechanical stirrer for 300 min and an ultrasonic treatment for 60 min (Fig. 7b) is higher than that of the uncured film treated with a mechanical stirrer for 300 min and grinder treatment for 720 min (Fig. 7a). These results also indicate that

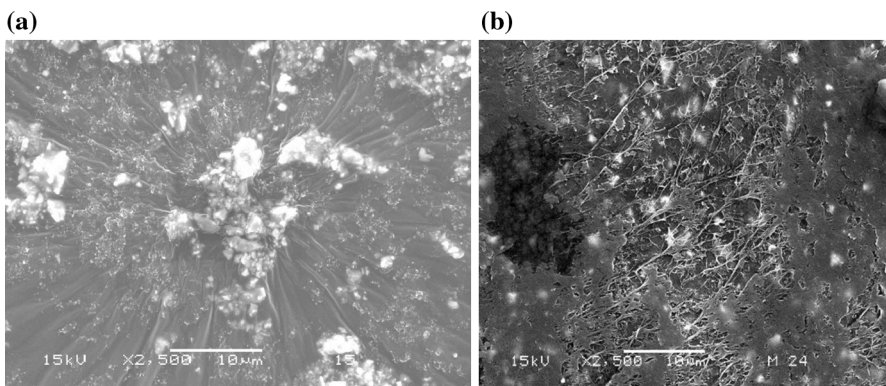


Fig. 6 SEM images of uncured epoxy/BC film with the absence of GS (a) and presence of GS (b)

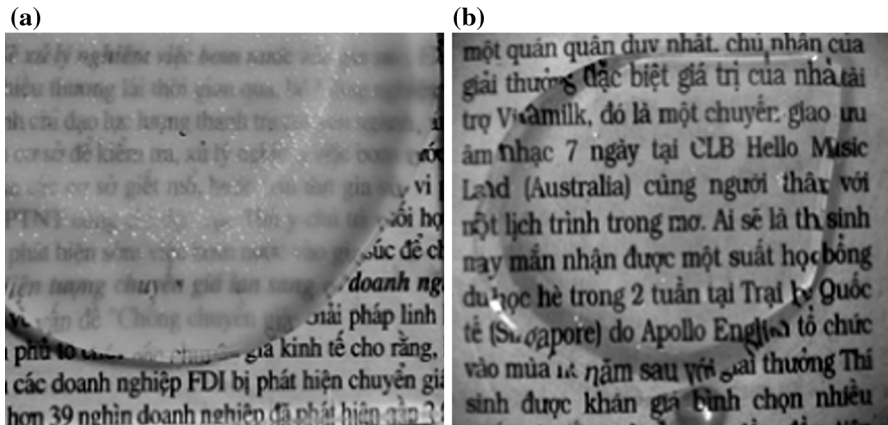


Fig. 7 Comparison of the optical transparency of uncured epoxy film received by combining mechanical stirrer and grinder treatment (a) and by combining mechanical stirrer and ultrasonication treatment (b)

by combining the mechanical stirrer and ultrasonication, the resulting BC/EP mixture showed a better dispersion of BC with single nanoscale fibers.

Curing processing of epoxy/BC mixture with MHPA catalyst

The effects of various factors, such as MHPA/EP molar ratios, curing temperature, NMI, and polyol contents, on the gel content and curing rate of the epoxy resin, were examined to determine the optimal curing conditions for the bio-based composite material fabrication.

In this experiment, the MHPA/EP molar ratios were used in the range from 1/0.8 to 1/1.05. The bio-based composite materials were processed at 120 °C in the presence of 1.5 wt% of NMI and polyol as accelerators. Figure 8a shows the relationship between the gel content and curing time.

When the proceeded curing time was shorter than 7 min, the effects of the MHPA/EP molar ratios on the gel content were negligible. The increasing trend of the gel content at higher molar ratios was observed when the curing time reached more than 10 min. On the other hand, when the MHPA/EP molar ratio reached 1.05, the gel content was similar to that with an equivalent ratio (MHPA/EP = 1). All samples almost reached the maximum gel content after 30 min under the curing conditions.

The relationship between curing rate and curing time was calculated and plotted in Fig. 8b based on the gel content and curing time.

The results showed that the curing rate increased with increasing MHPA/EP molar ratios. The curing rate showed no change when the MHPA/EP molar ratio was 1.05 compared to an equivalent ratio. All samples showed the maximum curing rate after 5 min. The curing temperature has a strong effect on the structure and mechanical characteristics of the epoxy resin. Generally, at high temperatures, the epoxy resin reached the maximum gel content at a short time with very brittle characteristics. Note that finding a suitable temperature for this process is essential.

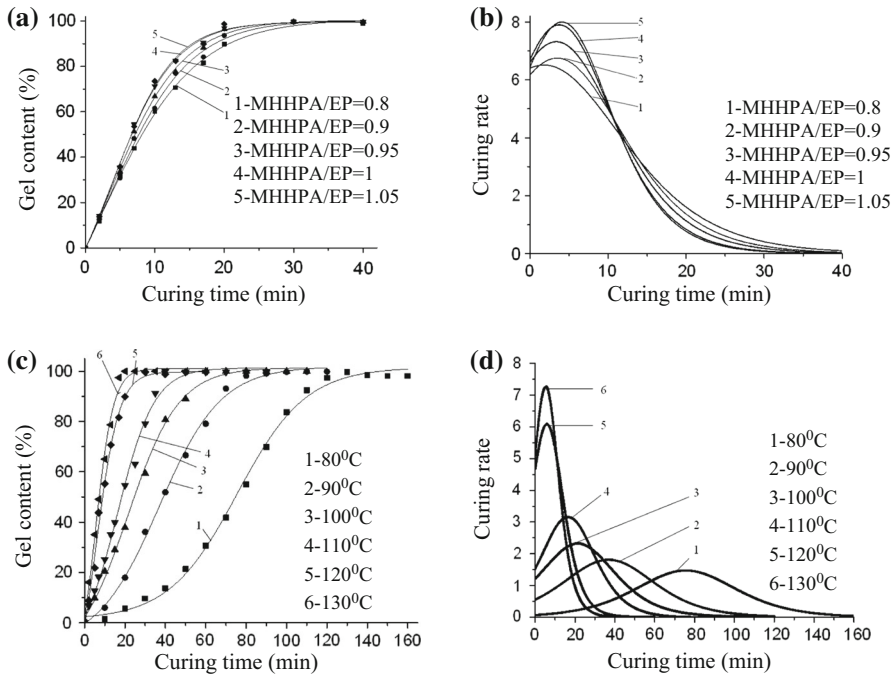


Fig. 8 Effect of MHHPA/EP molar ratios (a, b) and curing temperature (c, d) on gel content and curing rate of epoxy resin

The effects of the different curing temperature on the gel content and curing rate of epoxy resin was investigated, as shown in Fig. 8c.

All samples had an MHHPA/EP molar ratio of 0.8 in the presence of 1.5 wt% of both NMI and polyol. The results showed that when the curing temperature increased, the gel content reached higher values for a short time. The curing times for the maximum gel content at 80, 90, 100, 110, 120 and 130 °C were 130, 90, 60, 40, 30 and 17 min, respectively. Figure 8d also indicates the effect of the curing temperature on the curing rate of epoxy resin. At different curing temperatures, the time for the maximum gel content was different and longer when the temperature decreased.

In the curing processing of epoxy resin, the key role of NMI is as an accelerator that is greatly affected by both the gel content and curing rate. The effects of the NMI contents in the range 0–2 wt% at 100 °C and the MHHPA/EP molar ratio, 0.8, on the gel content and curing rate were also investigated, as shown in Fig. 9a, b.

The data in Fig. 9a, b suggests that the curing reaction did not occur in the absence of NMI, and the gel content was nearly zero. On the other hand, in the presence of only 0.5 wt% NMI, the curing reaction proceeded easily, and after 60 min the gel content reached approximately 80%. In the presence of 2 wt% NMI, the gel content reached a maximum for only 10 min. These results corroborate the curing rate results. The curing rate of the epoxy resin in the absence of NMI was

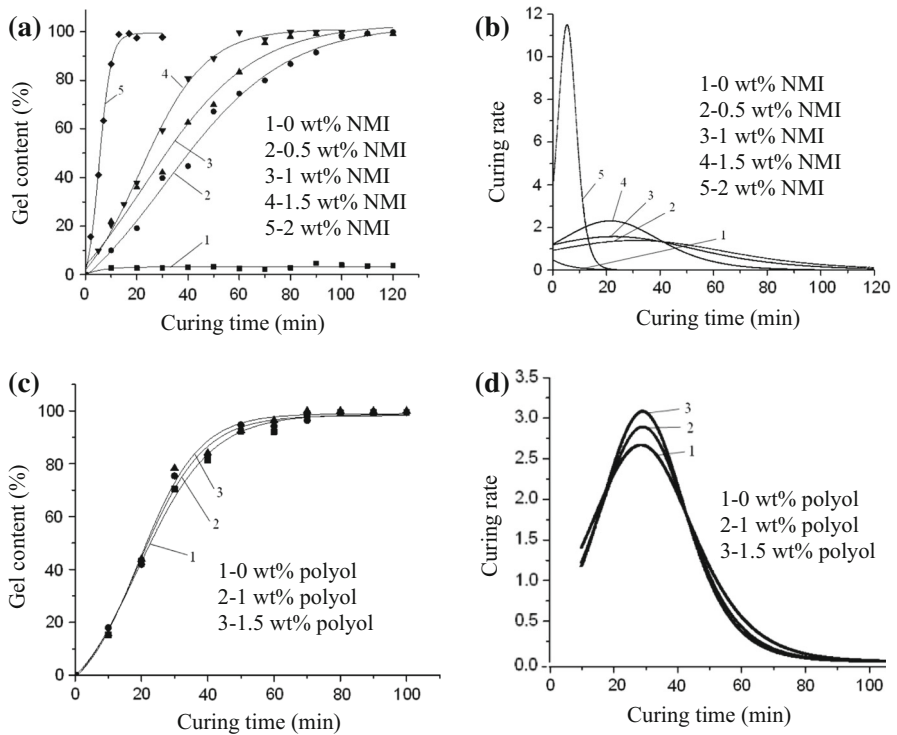


Fig. 9 Effect of NMI (a, b) and polyol (c, d) contents on gel content and curing rate of epoxy resin

zero and increased with increasing NMI content. At 2 wt% NMI, the curing rate of the epoxy resin reached the maximum value after 7 min.

Similar to NMI, polyol plays a vital role in the curing reaction of epoxy as an accelerator. Therefore, the effect of the polyol content on the gel content and curing rate of epoxy resin needs to be examined. Polyol was used in the range from 0 to 1.5 wt% with the other conditions fixed, such as temperature, NMI content and EP/MHHPA molar ratio of 100 °C 1.5 and 0.8 wt%, respectively. Figure 9c, d shows the relationship between both the gel content and curing rate with curing time. The curing rate increased with increasing polyol content.

Regarding the effect of the BC contents on the curing characteristics of epoxy, several curing parameters, such as curing temperature, MHHPA/EP molar ratio, NMI and polyol content were fixed at 100 °C, 0.8, 1.5 and 1.5 wt%, respectively. The results are also presented in Fig. 10.

The data showed that when the BC contents changed in the range from 0 to 0.3 wt%, the gel content of epoxy resin did not change significantly. After 40 min under the curing conditions, the gel content of all samples reached approximately 90%. The results also showed that the curing rate of the epoxy decreased with increasing BC content. At 0.3 wt% BC incorporation in EP, the maximum curing rate decreased significantly compared to the pristine epoxy due to the reduction of the

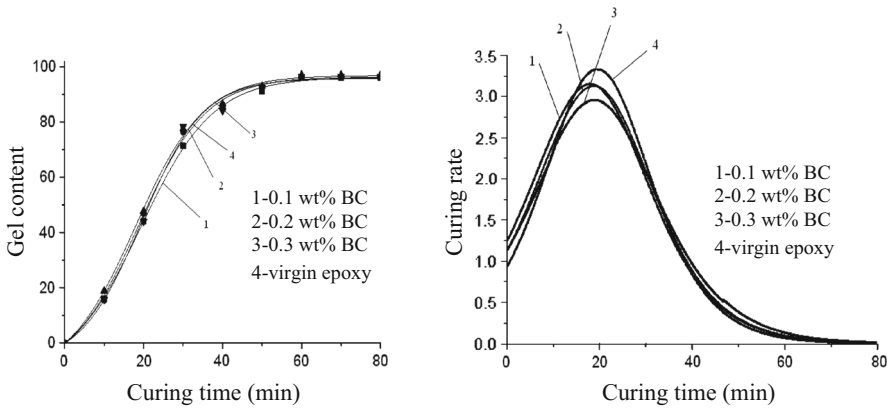


Fig. 10 Effect of BC contents on gel content and curing rate of epoxy resin

hydroxyl groups as the active group in the epoxy resin via formation of H bonds between the BC surface and epoxy resin.

Fracture toughness and mechanical characteristics of bio-based composites

Finding the optimal mechanical characteristics of epoxy resin as a matrix for fiber-reinforced polymer (FRP) is necessary due to the mechanical properties of FRP depending on not only the strength of the fiber, but also on the strength of the matrix. Therefore, this study focused on the effects of BC on the mechanical properties and fracture toughness of the epoxy resin. The fracture toughness parameters (critical stress intensity factor, K_{IC}) of the virgin epoxy and bio-based composite materials were calculated, as shown in Fig. 11.

The K_{IC} of the virgin epoxy was $0.5659 \text{ MPa m}^{1/2}$, revealing poor impact strength due to its inherent brittleness. This was overcome by the incorporation of

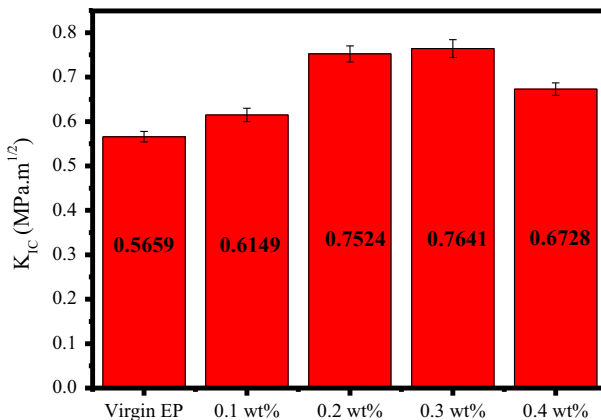


Fig. 11 Effect of BC loadings on K_{IC} value of epoxy resin

BC such that the fracture toughness was improved with a 0.3 wt% BC content. In addition, the K_{IC} was calculated to be $0.7641 \text{ MPa m}^{1/2}$, exhibiting the optimal K_{IC} of all BC-based formulations. On the other hand, at a higher loading of BC (0.4 wt%), the K_{IC} value started to decrease. The enhancement of the K_{IC} values in the presence of BC suggests that nanosized fiber BC prevents and changes the path of crack growth, which requires more energy. Such experimental results also agree with the morphological results of fracture surface of the epoxy resin.

Figure 12 shows the SEM images of the bio-composites in the presence and absence of 0.3 wt. % BC after the K_{IC} tests. As shown in Fig. 12a, b, the fracture surface of the virgin epoxy was smooth, which is typical for the fracture of brittle materials. Figure 12c, d shows rough fracture surfaces with numerous tortuous and fine river-like structures, suggesting that a large amount of energy was required to fracture the samples.

The effects of dispersion treatment methods, such as those (1) using a mechanical stirrer for 300 min (MS), (2) using both mechanical stirrer for 300 min and grinder for 720 min (MS + G) and (3) by combining the mechanical stirrer for 300 and 60 min of ultrasonication (MS + U), on the K_{IC} values were also investigated and the results are shown in Fig. 13.

In this test, the BC content was fixed to 0.3 wt% for all samples. All methods resulted in great improvement of the K_{IC} values compared to the virgin epoxy. The K_{IC} values corresponding to MS, MS + G and MS + U methods were 0.774,

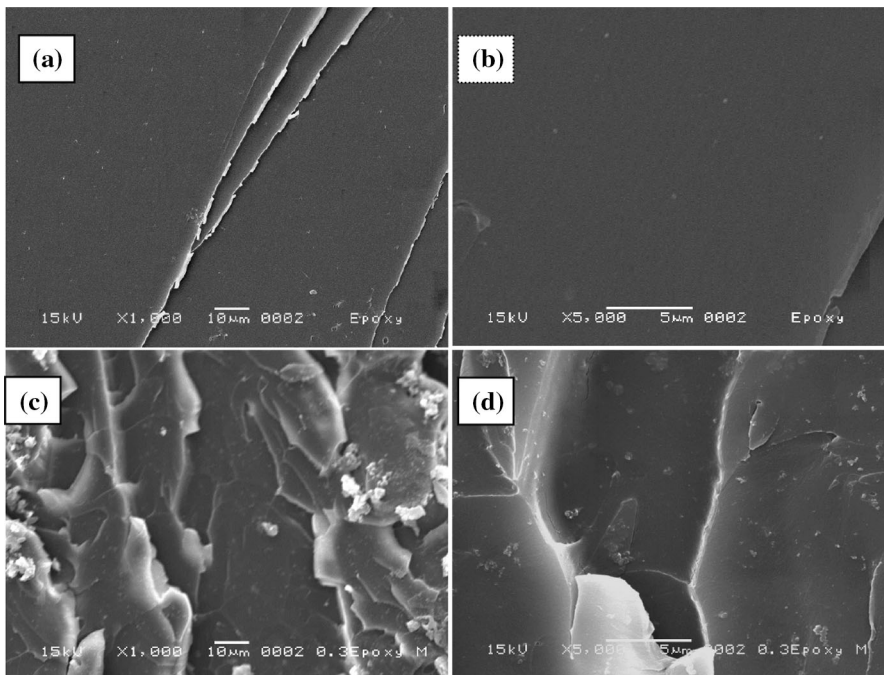


Fig. 12 SEM images of the fracture surface of neat epoxy (a, b) and epoxy/0.3 wt% BC-based composite (c, d)

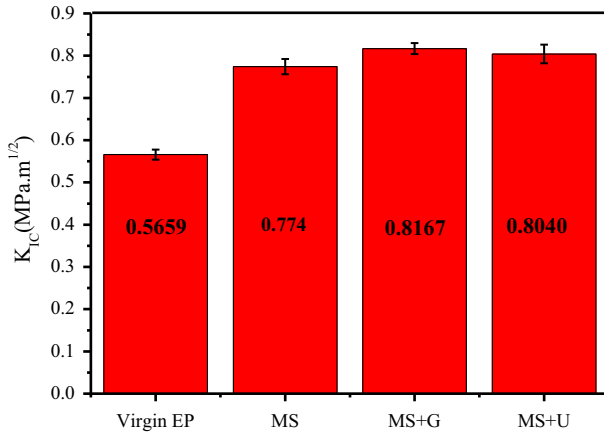


Fig. 13 Effect of dispersion methods on K_{IC} value of 0.3 wt% of BC in epoxy resin: (MS)—mechanical stirrer only, (MS + G)—mechanical stirrer for 300 min and grinder for 720 min, (MS + U)—mechanical stirrer with 300 and 60 min of ultrasonication

0.8167 and 0.8044, respectively. Based on these results, MS + U was chosen as the best method for incorporating BC into the epoxy matrix due to both the high transparency and K_{IC} value compared to the other methods. On the other hand, the dispersion of BC in the epoxy matrix received by this method depends greatly on the ultrasonic time. The effects of the ultrasonic times on the fracture toughness were also evaluated, as shown in Fig. 14.

The K_{IC} values of EP in the presence of 0.3 wt% of BC for 30 and 60 min ultrasonication were 0.7754 MPa m^{1/2} and 0.8044 MPa m^{1/2}, which was 37 and 42.1%, respectively, higher than that of the pristine epoxy. This was attributed to the good dispersion of all BC fibers in the epoxy resin.

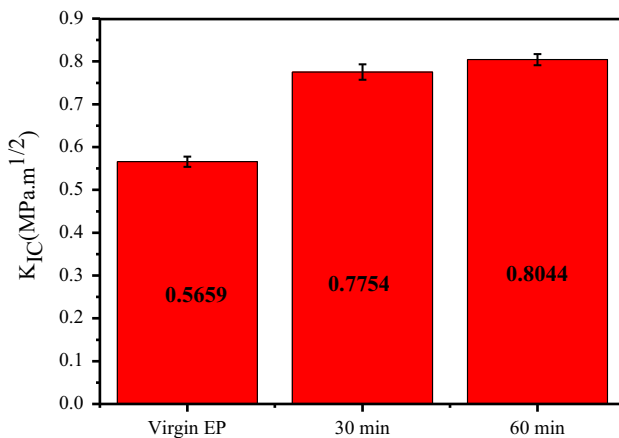


Fig. 14 Effect of ultrasonication times on K_{IC} value of epoxy resin: B1—neat epoxy, B2—0.3 wt% BC for 30 min of ultrasonication and B3—0.3 wt% BC for 60 min of ultrasonication

As discussed above, the surface of the BC fibers was treated with a silane coupling agent to enhance the compatibility between the BC and epoxy matrix. The most suitable silane compound for the epoxy resin should have an oxirane group in its structure. Therefore, the GS with a mono-oxirane group was chosen for this purpose. The curing agent can react with the oxirane group in both the GS and epoxy resin, which helps link the BC and epoxy chain. At higher contents, however, the silane compound will tend to aggregate on the BC surface and reduce these effects. Therefore, finding the optimal content of silane coupling agent is necessary. Figure 15 shows the effects of the silane contents from 0 to 3 wt% on the K_{IC} values of EP/BC 0.3 obtained by a mechanical stirring treatment for 300 min.

In the presence of GS, the K_{IC} values of the EP/BC 0.3 samples increased significantly compared to the case of the absence of GS. The prepared bio-composite with 2 wt% GS exhibited the optimal fracture toughness, $0.7740 \text{ MPa m}^{1/2}$, which was 36.8% higher than the sample in the absence of GS. On the other hand, at a higher GS content, about 3 wt%, the K_{IC} value decreased due to the relationship between the excessive content of GS and the structure of the cured epoxy resin as discussed above.

The effects of the BC contents on the mechanical properties of the epoxy resin, such as tensile and flexural properties, and impact strength were also examined. The bio-based composite materials comprising the BC contents (0–0.4 wt%), MHHPA and EP with an MHHPA/EP molar ratio of 0.8, NMI (1.5 wt%), polyol (1.5 wt%) and in the absence and presence of GS (2 wt%) were fabricated. The BC was well dispersed in the epoxy resin using both a mechanical stirrer for 300 min and ultrasonication for 60 min. The mechanical properties were examined after all the samples were stored at room temperature for 10 days, as listed in Table 1.

The results in Table 1 reveal the significant effects of GS on the tensile properties of cured EP/BC 0.3. The tensile strength of EP/BC 0.3 in the presence of 2 wt% GS was 9% higher compared to EP/BC 0.3 without GS and was 14.5% higher compared to virgin epoxy caused by the effects of GS on the good dispersion of BC in the

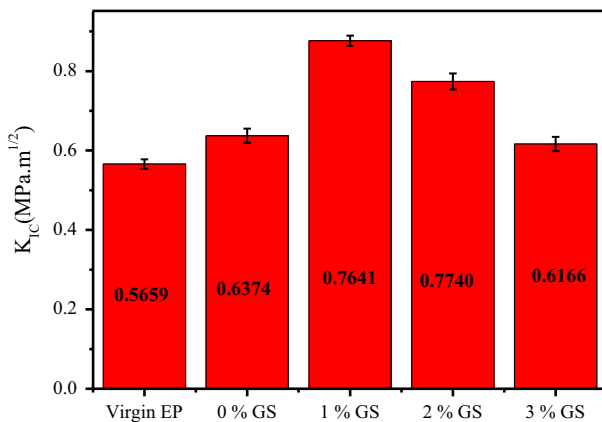


Fig. 15 Effect of silane coupling agents: 0% GS (EP/BC 0.3, 0 wt%), 1% GS (EP/BC 0.3, 1 wt %), 2% GS (EP/BC 0.3, 2 wt%) and 3% GS (EP/BC 0.3, 3 wt%) on fracture toughness of epoxy resin

Table 1 Effect of BC and GS contents on the mechanical characteristics of epoxy resin

Samples	Virgin epoxy	0.1 BC 2 GS	0.2 BC 2 GS	0.3 BC 2 GS	0.4 BC 2 GS	0.3 BC 0 GS
Tensile strength (MPa)	45.57	51.31	52.04	53.32	45.82	48.51
Tensile modulus (GPa)	1.45	1.52	1.53	1.68	1.43	1.57
Flexural strength (MPa)	72.58	79.04	78.52	83.05	69.03	75.32
Flexural modulus (GPa)	2.95	3.56	3.58	4.15	2.61	3.63
Impact strength (kJ/m ²)	7.52	6.23	6.78	7.29	6.32	5.05

epoxy resin. The same trend was also observed with the tensile modulus, and the tensile modulus was also increased slightly in the presence of GS.

The increasing trend of the flexural properties in the presence of GS was also confirmed. The flexural strength and flexural modulus of the epoxy in the presence of 2 wt% GS and 0.3 wt% BC (EP/BC 0.3) were 9.3–12.4% higher compared to the EP/BC 0.3 samples in the absence of GS. Both the tensile and flexural properties showed optimal values at 0.3 wt% BC in the epoxy resin and a decreasing trend with higher contents (0.4 wt%). The results of the impact test also indicated that the EP/BC 0.3 sample with 2 wt% of GS had higher values than the EP/BC 0.3 sample without GS, but the values did not change significantly when the BC contents were in the range 0.1–0.4 wt%. It is easy to realize that the fracture toughness which was obtained in this work was lower than the value of epoxy resin filled with nanosilica in Dittanet et al. [20] and thermal plastic resin in Jones et al. [22]; however, it was similar to epoxy filled and silica cured with anhydride or amine in Hsieh et al. [21]. This may be because the fracture toughness of the cured epoxy resin strongly depends on the type of epoxy, curing agent, reinforcement materials and fabrication methods.

Conclusions

This study examined the effects of nanosized BC fibers on the morphological and mechanical characteristics, and investigated the fracture toughness of epoxy-based biocomposites. The BC fabricated from an ethanol nata-de-coco suspension via an alkali pre-treatment, followed by solvent exchange was used for bio-based composite material preparation. The results indicated that BC enhanced the fracture toughness and mechanical properties due to the strong covalent bonds formed between the silane coupling agent and the fibers as well as between the silane coupling agent, epoxy resin and curing agent. This entailed a strong interface interaction between the fiber filler and epoxy matrix. Various factors affecting the

gel content and curing rate were also investigated. The fracture toughness, tensile strength and flexural strength of the composites with 0.3 wt% of BC and 2 wt% GS obtained by combining the mechanical stirrer for 300 min and 60 min of ultrasonication were $0.77641 \text{ MPa m}^{1/2}$, 53.3 MPa and 83.05 MPa, respectively. These values represent corresponding improvements of 35.0, 14.5 and 12.6% compared to the pristine epoxy.

References

1. Halder S, Ahemad S, Das S, Wang J (2016) Epoxy/Glass fiber laminated composites integrated with amino functionalized ZrO_2 for advanced structural applications. *ACS Appl Mater Interface* 8:1695–1706
2. Qin W, Vautard F, Askeland P, Yu J, Drzal L (2015) Modifying the carbon fiber–epoxy matrix interphase with silicon dioxide nanoparticles. *RSC Adv* 5:2457–2465
3. Micheli D, Vricella A, Pastore R, Delfini A, Giusti A, Albano M, Marchetti M, Moglie F, Primiani VM (2016) Ballistic and electromagnetic shielding behaviour of multifunctional Kevlar fiber reinforced epoxy composites modified by carbon nanotubes. *Carbon* 104:141–156
4. Sahoo SK, Mohanty S, Nayak SK (2015) Toughened bio-based epoxy blend network modified with transesterified epoxidized soybean oil: synthesis and characterization. *RSC Adv* 5:13674–13691
5. Kafy A, Akther A, Zhai L, Kim HC, Kim J (2017) Porous cellulose/graphene oxide nanocomposite as flexible and renewable electrode material for supercapacitor. *Synth Met* 223:94–100
6. Dayal MS, Catchmark JM (2016) Mechanical and structural property analysis of bacterial cellulose composites. *Carbohydr Polym* 144:447–453
7. Nguyen QT, Bandupriya HDD, Foale M, Adkins SW (2016) Biology, propagation and utilization of elite coconut varieties (makapuno and aromatics). *Plant Phys Biochem* 109:579–589
8. Nugroho DA, Aji P (2015) Characterization of Nata de Coco produced by fermentation of immobilized acetobacter xylinum. *Agric Agric Sci Proc* 3:278–282
9. Ullah H, Wahid F, Santos HA, Khan T (2016) Advances in biomedical and pharmaceutical applications of functional bacterial cellulose-based nanocomposites. *Carbohydr Polym* 150:330–352
10. Mueller S, Weder C, Foster EJ (2014) Isolation of cellulose nanocrystals from pseudostems of banana plants. *RSC Adv* 4:907–915
11. Saba N, Mohammad F, Pervaiz M, Jawaid M, Alothman OY, Sain M (2017) Mechanical, morphological and structural properties of cellulose nanofibers reinforced epoxy composites. *Int J Biol Macromol* 97:190–200
12. Guan F, Chen S, Yao J, Zheng W, Wang H (2016) ZnS/Bacterial Cellulose/Epoxy Resin (ZnS/BC/E56) nanocomposites with good transparency and flexibility. *J Mater Sci Technol* 32:153–157
13. Luddee M, Pivsa-Art S, Sirisansaneeyakul S, Pechyen C (2014) Particle size of ground bacterial cellulose affecting mechanical, thermal, and moisture barrier properties of PLA/BC biocomposites. *Energy Proc* 56:211–218
14. Blaker JJ, Lee KY, Walters M, Drouet M, Bismarck A (2014) Aligned unidirectional PLA/bacterial cellulose nanocomposite fibre reinforced PDLLA composites. *React Funct Polym* 85:185–192
15. Asgher M, Ahmad Z, Iqbal HMN (2017) Bacterial cellulose-assisted de-lignified wheat straw-PVA based bio-composites with novel characteristics. *Carbohydr Polym* 161:244–252
16. Qiao K, Zheng Y, Guo S, Tan J, Chen X, Li J, Xu D, Wang J (2015) Hydrophilic nanofiber of bacterial cellulose guided the changes in the micro-structure and mechanical properties of nf-BC/PVA composites hydrogels. *Compos Sci Technol* 118:47–54
17. Tang Y, Ye L (2015) A volume in Woodhead Publishing series in composites science and engineering. Woodhead Publishing, Sawston, Cambridge, pp 425–459
18. Mustata F, Tudorachi N, Rosu D (2012) Thermal behavior of some organic/inorganic composites based on epoxy resin and calcium carbonate obtained from conch shell of *Rapana thomasiana*. *Compos Part B* 43:702–710
19. Vu CM, Nguyen TV, Nguyen LT, Choi HJ (2016) Fabrication of adduct filled glass fiber/epoxy resin laminate composites and their physical characteristics. *Polym Bull* 73:1373–1391

20. Dittanet P, Pearson RA (2012) Effect of silica nanoparticle size on toughening mechanisms of filled epoxy. *Polymer* 53:1890–1905
21. Hsieh TH, Kinloch AJ, Masania K, Taylor AC, Sprenger S (2010) The mechanisms and mechanics of the toughening of epoxy polymers modified with silica nanoparticles. *Polymer* 51:6284–6294
22. Jones AR, Watkins CA, White SR, Sottos NR (2015) Self-healing thermoplastic-toughened epoxy. *Polymer* 74:254–261
23. Vu CM, Choi HJ (2016) Enhancement of interlaminar fracture toughness of carbon fiber/epoxy composites using silk fibroin electrospun nanofibers. *Polym Plast Technol Eng* 55:1048–1056
24. Liu S, Fan X, He C (2016) Improving the fracture toughness of epoxy with nanosilica-rubber core-shell nanoparticles. *Compos Sci Technol* 125:132–140
25. Ladani RB, Wu S, Kinloch AJ, Ghorbani K, Zhang J, Mouritz AP, Wang CH (2015) Improving the toughness and electrical conductivity of epoxy nanocomposites by using aligned carbon nanofibres. *Compos Sci Technol* 117:146–158
26. Boland CS, Barwich S, Khan U, Coleman JN (2016) High stiffness nano-composite fibres from polyvinylalcohol filled with graphene and boron nitride. *Carbon* 99:280–288
27. Son DR, Raghu AV, Reddy KR, Jeong HM (2016) Compatibility of thermally reduced graphene with polyesters. *J Macromol Sci Part B Phys* 55:1099–1110
28. Reddy KR, Lee KP, Gopalan AI (2007) Self-Assembly directed synthesis of poly (ortho-toluidine)-metal (gold and palladium) composite nanospheres. *J Nanosci Nanotechnol* 7:3117–3125
29. Han SJ, Lee HI, Jeong HM, Kim BK, Raghu AV, Reddy KR (2014) Graphene modified lipophilically by stearic acid and its composite with low density polyethylene. *J Macromol Sci Part B Phys* 53:1193–1204
30. Reddy KR, Hassan M, Gomes VG (2015) Hybrid nanostructures based on titanium dioxide for enhanced photocatalysis. *Appl Catal A Gen* 489:1–16
31. Reddy KR, Sin BC, Ryu KS, Kim JC, Chung H, Lee Y (2009) Conducting polymer functionalized multi-walled carbon nanotubes with noble metal nanoparticles: synthesis, morphological characteristics and electrical properties. *Synth Met* 159:595–603
32. Reddy KR, Karthik KV, Prasad SBB, Soni SK, Jeong HM, Raghu AV (2016) Enhanced photocatalytic activity of nanostructured titanium dioxide/polyaniline hybrid photocatalysts. *Polyhedron* 120:169–174
33. Khan MU, Reddy KR, Snguanwongchai T, Haque E, Gomes VG (2016) Polymer brush synthesis on surface modified carbon nanotubes via in situ emulsion polymerization. *Colloid Polym Sci* 294:1599–1610
34. Kim JH, Park S, Kim H, Kim HJ, Yang YH, Kim YH, Jung SK, Kan E, Lee SH (2017) Alginate/bacterial cellulose nanocomposite beads prepared using *Gluconacetobacter xylinus* and their application in lipase immobilization. *Carbohydr Polym* 157:137–145